23rd International Symposium on Mathematical Theory of Networks and Systems
Hong Kong University of Science and Technology, Hong Kong, July 16-20, 2018

Anti-windup scheme for networked proportional-integral control

Hamed Sadeghi, Richard Pates and Anders Rantzer

Abstract— **We propose an anti-windup scheme for a class of control problems. This class, includes networked systems, where each node contains a subsystem and each edge comprise a control action. The networked anti-windup control system is proposed to address the issues caused by integrator state saturation. We show that the suggested control scheme is input-output stable. Furthermore, we provide a numerical method for robust performance analysis of the suggested control system.**

Index Terms—**Distributed control, decentralized control, anti-windup, structure preserving.**

I. INTRODUCTION

When a system has many separate decision making units and their control actions must be determined based on partial (rather than total) information, it can be considered as a distributed control system. Due to their complexity and growing size, it is of great importance to have efficient methods for synthesis and implementation of distributed controllers.

An efficient approach to deal with distributed control problem of large-scale systems is to develop scalable and structure preserving control algorithms. Based on the concept of positive systems, a scalable method is introduced in [1]-[3], where it is shown that considering positive systems simplifies the synthesis of distributed controllers. Other scalable approaches are shown to be efficient in [4]-[5], where methods are suggested to design decentralized controller based on local information. For a survey of recent works in the area of distributed control, see [6].

In practice, all control systems deal with constraints. One type of practically common and important constraints, is the constraint due to control input limits, known as actuator saturation. For example, pumps have bounded flow capacity, motors have finite speed and torque and valves work in the range of fully open and fully closed states. These type of physical limitations, exist in all controlled systems, regardless of the control algorithm being centralized or decentralized. Hence, in applications we have to encounter with control signal constraints.

Recently, an H-infinity optimal static state feedback law is proposed in [7], where the control law is applicable to linear time-invariant systems with symmetric and Hurwitz state matrix. However, that control law is unable to remove stationary errors in presence of constant disturbance. To overcome that deficiency, an optimal H-infinity PI controller is developed in [8]. Specifically, the following problem was studied in the network context.

Consider a graph ($\mathscr{V}$, $\mathscr{E}$) where $\mathscr{V}$ and $\mathscr{E}$ are the sets of edges and nodes respectively. Associate with this graph the following system

$$\begin{cases} \dot{x}_i = a_i x_i(t) + \sum_{(i,j)\in\mathscr{E}} (u_{ij} + d_i) \\ e_i = r_i - x_i \end{cases} \tag{1}$$

where x_i is the state variable of the i-th subsystem with $i \in \mathscr{V}$, $a_i < 0$, $u_{ij} = -u_{ji}$. Moreover u, d, r and e are control-, disturbance-, reference- and error-signals respectively.

Given the above network system, the optimal state feedback control law that minimizes the $\mathbf{L}_2$-gain from r to u while keeping the $\mathbf{L}_2$-gain from d to integral of x bounded, is given by

$$\begin{cases} \dot{y}_{ij} = \kappa(e_i/a_i - e_j/a_j) \\ u_{ij} = y_{ij} - e_i/a_i^2 + e_j/a_j^2 \end{cases} \tag{2}$$

where κ is a gain. This control algorithm is clearly a decentralized (proportional-integral) control law, as the control action u_{ij} is determined by the error (and its integral) at the nodes i and j. In Figure 1 an example of a buffer network with the PI control (2) is depicted.

Now again we consider system (1), but this time with constraint on the control signal. Then the plant can be described as

$$\begin{cases} \dot{x}_i = a_i x_i(t) + \sum_{(i,j)\in\mathscr{E}} (\mathrm{sat}(v_{ij}) + d_i) \\ e_i = r_i - x_i \end{cases} \tag{3}$$

where sat(.) denotes the saturation unit and v is the control signal. Here as a result of the introduced saturation, system (3) with controller (2) exhibits integrator windup phenomenon. To address that issue, we suggest the following control law

$$\begin{cases} e_{s,ij} = \mathrm{sat}(v_{ij}) - v_{ij} \\ \dot{y}_{ij} = \kappa(e_i/a_i - e_j/a_j) + f e_{s,ij} \\ v_{ij} = y_{ij} - e_i/a_i^2 + e_j/a_j^2 \end{cases} \tag{4}$$

where y is the integrator state, f is the anti-windup feedback gain and e_s is the saturation error and defined as the difference between the output of saturation unit and the control signal, that is $e_s = \mathrm{sat}(v) - v$. The saturation error is zero whenever the control signal v is within the saturation limits

This work was partially supported by the Wallenberg Artificial Intelligence, Autonomous Systems and Software Program (WASP) funded by Knut and Alice Wallenberg Foundation. The authors are members of the LCCC Linnaeus Center and the ELLIIT Excellence Center at Lund University.

The authors are with the Department of Automatic Control, Lund University, Box 118, SE-222 00 Lund, Sweden. ({hamed.sadeghi, richard.pates, anders.rantzer}@control.lth.se)

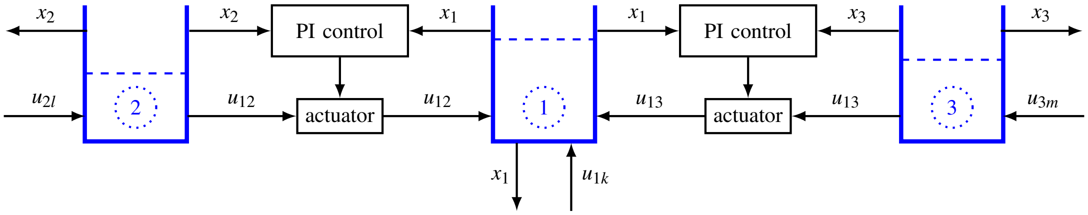

Fig. 1. A buffer network with distributed PI control (2), where x_i is the level in the buffer i and u_{ij} is the control signal between the buffers i and j. The unlinked arrows illustrate where the connections are to the rest of the network.

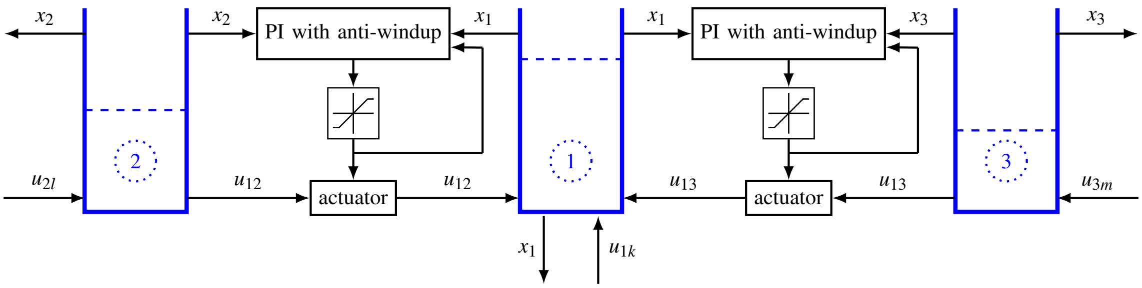

Fig. 2. A buffer network with distributed PI control equipped with the proposed anti-windup scheme (4). The unlinked arrows illustrate where the connections are to the rest of the network.

and is nonzero otherwise. When integrator windup happens, control signal will be saturated and hence the anti-windup becomes activated. Therefore, the saturation error signal is fed to the integrator state through the anti-windup gain f. This prevents the integrator from winding up. The rate at which the controller output is affected by the anti-windup feedback loop, is determined by the anti-windup feedback gain, f, where $1/f$ can be interpreted as the time constant of the anti-windup feedback loop. It is worth mentioning that the control signal v_{ij} is determined by the errors at the nodes i and j and by the saturation error of the neighbouring nodes. Hence, this control algorithm is a decentralized control law. An example of a buffer network with the anti-windup control scheme (4) is illustrated in Figure 2.

The outline of the paper is as follows. We summarize the notations in section II. In section III, we propose an anti-windup scheme is to address the problem of control signal saturation for a class of dynamic state-feedback control systems. Besides showing input-output stability, a numerical robust performance analysis is given in that section. In section IV, we provide a basic numerical example to show an application of the results. Concluding remarks is given in section V.

II. Notation

Let $\mathbf{L}_2$ be the set of square integrable functions $u : [0,\infty) \longrightarrow \mathbb{R}$ and $\mathbf{L}_{2e}$ the set of functions $u : [0,\infty) \longrightarrow \mathbb{R}$ that need only be square integrable on finite intervals. An operator $H : \mathbf{L}_{2e}^m \longrightarrow \mathbf{L}_{2e}^n$ is said to be bounded if the operator norm

$$\|H\| = \sup\{\frac{\|H(u)\|}{\|u\|} : u \in \mathbf{L}_2^m, u \neq 0\}$$

is finite. We say an operator H is casual, if $P_T H = P_T H P_T$ where P_T is the past projection operator which leaves a function unchanged on the interval $[0,T]$, and gives the value zero everywhere else. Corresponding transfer function of a linear time-invariant operator H is represented by $\hat{H}(s)$. Furthermore, Fourier transformation of a signal v is denoted by $\hat{v}$. Moreover, the scalar saturation operator is denoted by δ.

For a matrix $M \in \mathbb{R}^{n\times m}$, pseudo-inverse and spectral norm of M is denoted by $M^\dagger$ and $\|M\|$ respectively.

III. Results

In this section, we first give a summary of the main result of [8] to build the ground for the rest of this paper.

Consider the system depicted in Figure 3, with

$$\hat{P}(s) = (sI - A)^{-1}B \tag{5}$$

where $\hat{K}$ is the controller, A is the state matrix and assumed to be symmetric and negative definite, and B is a full rank matrix. The optimal state feedback control law that minimizes the $\mathbf{L}_2$-gain from r to u while keeping the $\mathbf{L}_2$-gain from d to integral of x bounded by $\tau \geq \sqrt{\|B^T A^{-4} B\|}$, is given in [8], in the form of a distributed PI controller

$$\hat{K}(s) = K_p + \frac{1}{s}K_i \tag{6}$$

with the following gains

$$K_p = \kappa B^T A^{-2} \tag{7}$$

$$K_i = -\kappa B^T A^{-1} \tag{8}$$

where κ is the gain below

$$\kappa = \left\| \frac{1}{\tau}(A^{-1}B)^\dagger \right\|. \tag{9}$$

We can see that due to the particular form of the controller gain matrices K_p and K_i, if matrix A is diagonal then the sparsity pattern of the controller will be similar to the sparsity pattern of B^T. This property leads to scalability characteristic of the controller, specially when B is the incidence matrix describing structure of the network.

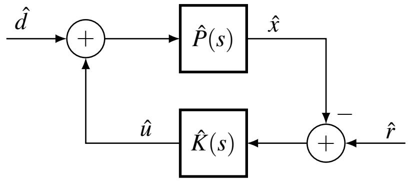

Fig. 3. Block diagram of the system described in (5)-(6), with process disturbance $\hat{d}$, reference input $\hat{r}$, control signal $\hat{u}$, plant output $\hat{x}$, controller $\hat{K}$ and process $\hat{P}$.

When it comes to the controller realization, depending on the size of $B \in \mathbb{R}^{n \times m}$, there are two interpretations based on the number of integrators. In the associated graph of the system, n and m correspond to the number of the nodes and the edges respectively. In the case that B^T has more rows than columns ($m \geq n$), it is better to describe the controller realization as the following

$$u(t) = \kappa B^T A^{-2} e(t) - \kappa B^T A^{-1} \int_0^t e(\xi) d\xi$$

hence, we need to have n integrator in the controller. On the other hand, if B^T has more columns than rows ($n = m+1$), it is more efficient to consider the following realization of the controller

$$u(t) = \kappa B^T A^{-2} e(t) - \int_0^t \kappa B^T A^{-1} e(\xi) d\xi$$

that is, we need to have m integrators in the controller in this case.

With the above described realization of the controller, we always have the minimal number of the integrators. In this paper for simplicity, we consider the second realization of the controller which corresponds to a tree-structured graph.

As already mentioned, in presence of integrator in the control law, windup problem is likely to happen. To avoid the negative effects of integrator windup, the following anti-windup scheme is proposed.

$$\begin{cases} w = \Delta(v) \\ e_s = w - v \\ e = r - x \\ \dot{y} = K_i e + F e_s \\ v = y + K_p e \end{cases} \tag{10}$$

where v is the control signal, w is the output of the saturation unit, e_s is the saturation error and defined as $e_s = w - v$, e is the error signal, and K_p and K_i are given by (7) and (8) respectively. Moreover, F is the anti-windup gain matrix and Δ is a nonlinear casual operator, consisting of scalar saturation elements δ_i acting on the signal v_i

$$\Delta = \begin{bmatrix} \delta_1 & & \\ & \ddots & \\ & & \delta_n \end{bmatrix} \tag{11}$$

The anti-windup control system is illustrated in Figure 4.

The rest of this section, is devoted to show the stability and evaluate the performance of the anti-windup scheme.

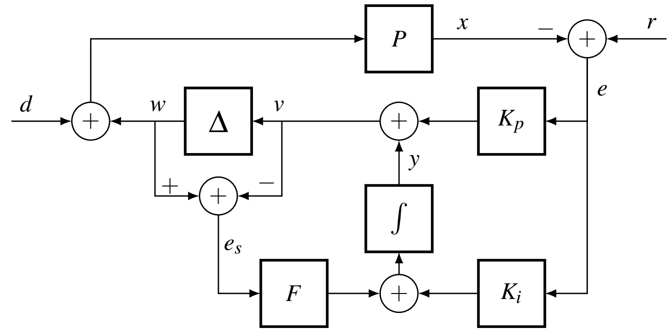

Fig. 4. The proposed anti-windup control, with saturation block Δ, anti-windup gain matrix F, proportional gain K_p, integral gain K_i, and the integrator state defined as y. This anti-windup model is similar to the well-known back calculation anti-windup scheme.

A. Stability analysis

To show input-output stability of the feedback system in Figure 4, we use circle criterion in integral quadratic constraint (IQC) framework, this will facilitate the performance analysis in the end of this section. To use that approach, we state the control system in Figure 4, with the following feedback configuration

$$\begin{cases} v = Gw + d_2 \\ w = \Delta(v) + d_1 \end{cases} \tag{12}$$

where d_1 and d_2 are interconnection noise and G is a casual linear time-invariant operator with the transfer function

$$\hat{G}(s) = (F + sI)^{-1}(F - \kappa B^T A^{-2} B) \tag{13}$$

and Δ is a nonlinear operator with bounded gain defined in (11). The interconnection (12), is graphically demonstrated in Figure 5. We say that the feedback system in (12) is stable if there exist a constant $C > 0$ such that

$$\int_0^T (|v|^2 + |w|^2) dt \leq C \int_0^T (|d_1|^2 + |d_2|^2) dt$$

for any $T \geq 0$.

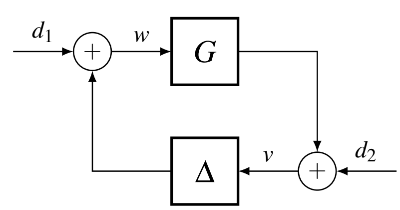

Fig. 5. Studied feedback configuration. d_1 and d_2 belong to $\mathbf{L}_{2e}$ and represent interconnection noise. G and Δ are linear and nonlinear casual operators respectively.

Input-output stability of the proposed anti-windup control system follows from stability of the feedback interconnection in (12).

Theorem 1. *Let $A \in \mathbb{R}^{n\times n}$ be a symmetric and negative definite matrix, $B \in \mathbb{R}^{n\times m}$ be a full-rank matrix and κ be the gain defined in* (9)*. Consider the feedback system described by* (10)-(13)*. If the anti-windup gain matrix is $F = fI$ with $f > 0$, then the feedback interconnection is input-output stable.*

Proof: It is straightforward to verify that the IQC below

$$\int_{-\infty}^{\infty} \begin{bmatrix} \hat{v}(j\omega) \\ \hat{w}(j\omega) \end{bmatrix}^* \Pi \begin{bmatrix} \hat{v}(j\omega) \\ \hat{w}(j\omega) \end{bmatrix} d\omega \geq 0$$

with the multiplier

$$\Pi = \begin{bmatrix} 0 & I \\ I & -2I \end{bmatrix}$$

holds for any $\hat{w} = \Delta(\hat{v})$. If

$$\begin{bmatrix} \hat{G}(j\omega) \\ I \end{bmatrix}^* \Pi \begin{bmatrix} \hat{G}(j\omega) \\ I \end{bmatrix} < 0 \qquad \forall \omega \in \mathbb{R} \tag{14}$$

holds, then input-outpout stability of (12) follows [9]. Substituting Π into inequality (14), gives

$$\hat{G}(j\omega)^* + \hat{G}(j\omega) - 2I < 0 \quad \forall \omega \in \mathbb{R}$$

replacing $\hat{G}(j\omega)$ from (13), yields

$$\frac{fI - \kappa B^T A^{-2} B}{f + j\omega} + \frac{fI - \kappa B^T A^{-2} B}{f - j\omega} - 2I < 0 \quad \forall \omega \in \mathbb{R}$$

after simplification we get

$$-f\kappa B^T A^{-2} B - \omega^2 I < 0 \quad \forall \omega \in \mathbb{R}$$

which is obviously true, since $B^T A^{-2} B$ is a positive definite matrix. Hence the theorem is proved. □

B. Robust performance analysis

To evaluate robust performance of the system, we use the method described in [10]. To do so, we need to reconfigure the system to the linear fractional transformation (LFT), illustrated in Figure 6. The equivalent algebraic representation can be written as

$$\begin{cases} \begin{bmatrix} z \\ v \end{bmatrix} = G \begin{bmatrix} e \\ w \end{bmatrix} \\ w = \Delta(v) \end{cases} \tag{15}$$

where G is a stable LTI system, Δ is the saturation block, z is the controlled variable and e is the exogenous input. One of the most common performance indices in robust analysis is the $\mathbf{L}_2$-gain of the system. As we want to investigate robust $\mathbf{L}_2$-performance of the system, we consider its corresponding IQC below

$$\int_0^{\infty} (|z(t)|^2 - \gamma^2 |e(t)|^2) dt \leq 0$$

To show that the system has robust $\mathbf{L}_2$-gain γ, it is sufficient to show that the following frequency domain inequality (FDI) holds

$$\begin{bmatrix} \hat{G}(j\omega) \\ I \end{bmatrix}^* M \begin{bmatrix} \hat{G}(j\omega) \\ I \end{bmatrix} \leq 0 \tag{16}$$

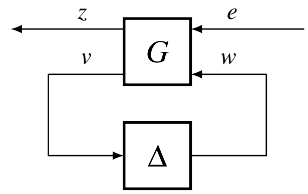

Fig. 6. Graphical illustration of the linear fractional transformation in relation (15).

for $\omega \geq 0$, where $\hat{G}$ is the transfer function of operator G and

$$M = \begin{bmatrix} I & 0 & 0 & 0 \\ 0 & \Pi_{11} & 0 & \Pi_{12} \\ 0 & 0 & -\gamma^2 I & 0 \\ 0 & \Pi_{12}^* & 0 & \Pi_{22} \end{bmatrix}$$

with $\Pi_{11} = 0$, $\Pi_{12} = \tau I$, $\Pi_{12} = -2\tau I$, and $\tau > 0$.

To investigate the robust performance of the anti-windup control system, we consider two cases. First, the map from the reference input r to the control signal v, and then, the map from the disturbance d to the integrator state y. In the first case $z = v$ and $e = r$ and in the later case, $z = y$ and $e = d$. To carry out the analysis, next we find what the map G is for each case. The transfer matrix of the first case is

$$\hat{G}_1(s) = (sI + F)^{-1} \begin{bmatrix} s\hat{K} & F - s\hat{K}P \\ s\hat{K} & F - s\hat{K}P \end{bmatrix}$$

and the the map for the second case is found to be

$$\hat{G}_2(s) = (sI + F)^{-1} \begin{bmatrix} (FK_p - K_i)P & F + (FK_p - K_i)P \\ -s\hat{K} & F - s\hat{K}P \end{bmatrix}$$

To find γ, one way is to verify the FDI in (16). Instead, in a more efficient way, we can use Kalman-Yakubovich-Popov (K-Y-P) lemma [11], to find the corresponding linear matrix inequality (LMI) and then verify it. To do so, we should have the corresponding state space description of the transfer matrices $\hat{G}_1(s)$ and $\hat{G}_2(s)$. Assume that $\hat{G}(s) = \tilde{C}(sI - \tilde{A})^{-1}\tilde{B} + \tilde{D}$. Then according to K-Y-P lemma, if M is a real matrix and (16) is satisfied, then there exists a real matrix $P = P^T$ such that the following LMI holds

$$\tilde{M} + \begin{bmatrix} \tilde{A}P + P\tilde{A} & P\tilde{B} \\ \tilde{B}^T P & 0 \end{bmatrix} \leq 0 \tag{17}$$

where

$$\tilde{M} = \begin{bmatrix} \tilde{C} & \tilde{D} \\ 0 & I \end{bmatrix}^T M \begin{bmatrix} \tilde{C} & \tilde{D} \\ 0 & I \end{bmatrix}$$

hence we can claim that the system has robust $\mathbf{L}_2$-gain γ.

It should be noted that, when we deal with large systems, the LMI in (17) gets large and it cannot be verified efficiently. However, there are methods suggested in the literature such as in [12] to help efficiently validating the LMI's that have sparsity pattern. This issue of scalability could be addressed either by introducing efficient methods to verify the LMI's or by finding an analytic upper bound for $\mathbf{L}_2$ performance of the system. This is left as a future research direction.

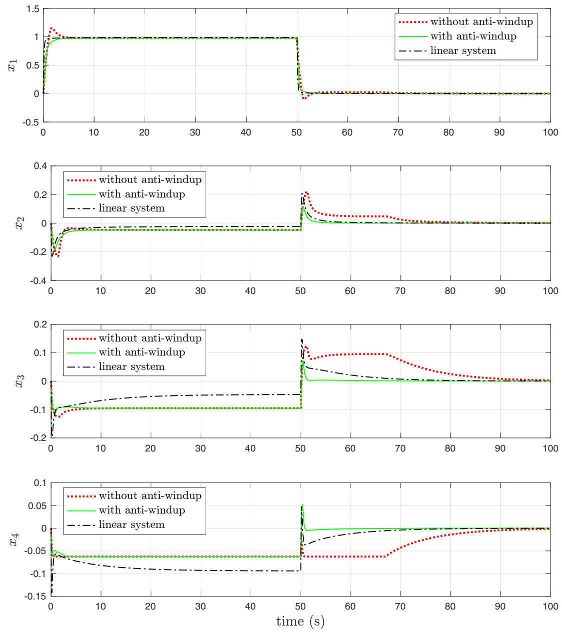

Fig. 7. State variables in response to the reference input $r = \begin{bmatrix}\mathbf{1}(t)-\mathbf{1}(t-50) & 0 & 0 & 0\end{bmatrix}^T$ for the system with and without anti-windup scheme and the linear case.

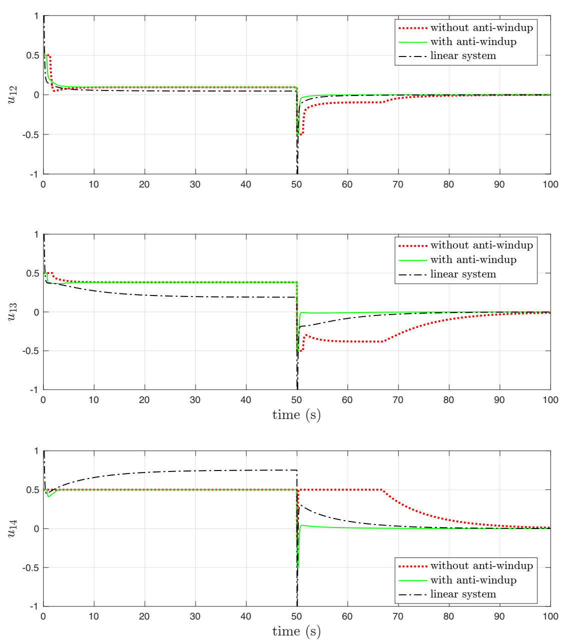

Fig. 8. Control signals in response to the reference input $r = \begin{bmatrix}\mathbf{1}(t)-\mathbf{1}(t-50) & 0 & 0 & 0\end{bmatrix}^T$ for the system with and without anti-windup scheme and the linear case.

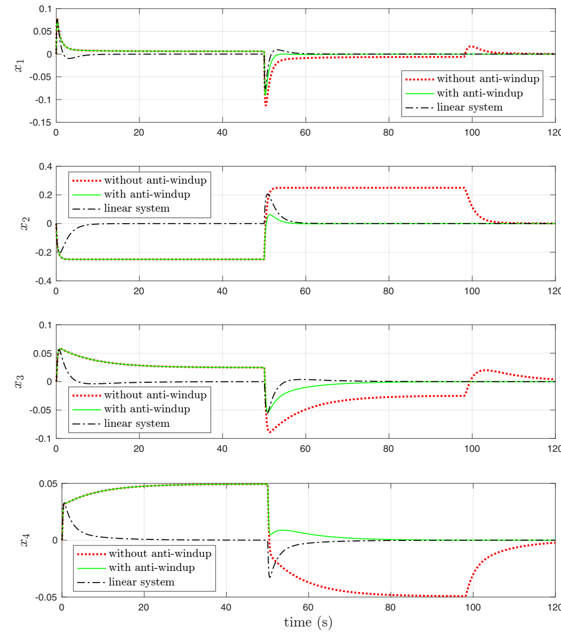

Fig. 9. State variables in response to the load disturbance $d = (\mathbf{1}(t) - \mathbf{1}(t-50))\begin{bmatrix}1 & -1 & 0 & 0\end{bmatrix}^T$ for the system with and without anti-windup control and the linear case.

IV. Example and Discussion

Consider a buffer system with four buffers connected in star configuration (see Figure 1). The following state space model

$$\begin{bmatrix}\dot{x}_1\\ \dot{x}_2\\ \dot{x}_3\\ \dot{x}_4\end{bmatrix} = A\begin{bmatrix}x_1\\ x_2\\ x_3\\ x_4\end{bmatrix} + B\begin{bmatrix}u_{12}\\ u_{13}\\ u_{14}\end{bmatrix} + \begin{bmatrix}d_1\\ d_2\\ d_3\\ d_4\end{bmatrix} \tag{18}$$

with

$$A = -\mathrm{diag}([1,2,4,8]), \quad B = \begin{bmatrix}1 & 1 & 1\\ -1 & 0 & 0\\ 0 & -1 & 0\\ 0 & 0 & -1\end{bmatrix}$$

describes the dynamics of the levels in the buffers, where x_i is the level (difference with some steady state) in the buffer i, d_i is the disturbance to the buffer i, and u_{ij} is the control signal between the buffers i and j. We want to attain a specific level in each of the buffers while disturbance is being rejected to a certain extent.

To evaluate performance of the system with the anti-windup controller, a simulation is carried out and the results are illustrated in Figures 7 to 10. In each case, a square signal $(\mathbf{1}(t) - \mathbf{1}(t-50))$ is applied to the system to evaluate the systems behaviour when the applied signal changes. In Figures 7 and 8, it can be seen that in response to a reference change, the system without anti-windup control, exhibits overshoot and undershoot as a result of control

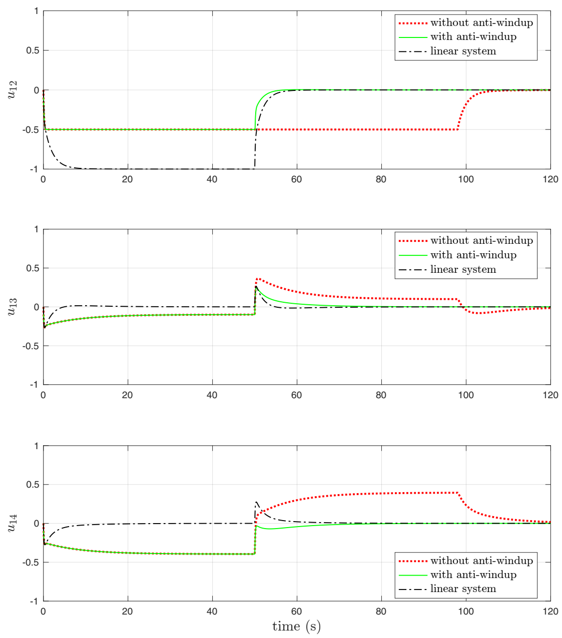

Fig. 10. Control signals in response to the load disturbance $d = (\mathbf{1}(t) - \mathbf{1}(t-50))\begin{bmatrix}1 & -1 & 0 & 0\end{bmatrix}^T$ for the system with and without anti-windup control and the linear case.

signal saturation. In Figures 9 and 10, we can see for the system without anti-windup, there is a considerable amount of delay before the control signal returns within the saturation range. Hence there is a delay in the response of state variables to the change of disturbance input. However, the the system with anti-windup control, doesn't exhibit this behaviour and recover quickly from being saturated.

Now we compare the $\mathbf{L}_2$-gain of the anti-windup control system with the linear case in [8]. To do so, consider the map from the reference input r to the control signal v (the signal which goes to the plant). For the specific example provided in here, in the linear case, $\mathbf{L}_2$-gain of the system is 5.16, while for the anti-windup control system, an upper bound to the same performance measure is larger and found to be 9.01. To find the upper bound of $\mathbf{L}_2$-gain for the nonlinear case, a minimization over f is carried out.

It is not surprising that there is a gap between upper bound of $\mathbf{L}_2$-gain of the anti-windup system and $\mathbf{L}_2$-gain of its linear counterpart. However, the method that we used could be conservative and this issue could be addressed by using a family of multipliers in the IQC method. That is, instead of choosing a single multiplier, we could have solved an optimization problem over a family of multipliers which satisfy the IQC defined by saturation (Δ), to find a better linear combination of valid multipliers. In this way, the mentioned gap would be smaller.

Similarly for the map from the disturbance d to the integrator state y, the upper bound of the $\mathbf{L}_2$-gain is evaluated for this numerical example. For that case, the upper bound is found to be 4.25. Existence of the upper bound of the $\mathbf{L}_2$-gain, shows that for the worst case disturbance, the integrator state and therefore the control signal will remain bounded.

V. Conclusions and Future Works

We proposed an anti-windup scheme for a class of networked control systems. The suggested anti-windup control system addresses the control signal saturation problem caused by the integrator windup. As this work is built upon a structure preserving PI controller, the proposed anti-windup scheme is also structure preserving. Moreover, using circle criterion for a special yet important class of anti-windup control systems, we showed that the system is input-output stable. Furthermore, we presented a numerical method for robust performance analysis.

Generalizing the proof of stability and providing a closed form expression for the $\mathbf{L}_2$-gain of the system can be done in the next line of research. Moreover, a design criterion for the anti-windup gain can be found using robust analysis, which is also left as a future research direction.

References

[1] Rantzer A. Scalable control of positive systems. European Journal of Control. 2015 Jul 31;24:72-80.
[2] Tanaka T, Langbort C. The bounded real lemma for internally positive systems and H-infinity structured static state feedback. IEEE transactions on automatic control. 2011 Sep;56(9):2218-23.
[3] Rantzer A. Distributed control of positive systems. In Decision and Control and European Control Conference (CDC-ECC), 2011 50th IEEE Conference on 2011 Dec 12 (pp. 6608-6611). IEEE.
[4] Pates R, Vinnicombe G. Scalable Design of Heterogeneous Networks. IEEE Transactions on Automatic Control. 2017 May;62(5):2318-33.
[5] Wang YS, Matni N, You S, Doyle JC. Localized distributed state feedback control with communication delays. In American Control Conference (ACC), 2014 2014 Jun 4 (pp. 5748-5755). IEEE.
[6] Mahajan A, Martins NC, Rotkowitz MC, Yksel S. Information structures in optimal decentralized control. In Decision and Control (CDC), 2012 IEEE 51st Annual Conference on 2012 Dec 10 (pp. 1291-1306). IEEE.
[7] Lidstrom C, Rantzer A. Optimal H state feedback for systems with symmetric and Hurwitz state matrix. In American Control Conference (ACC), 2016 2016 Jul 6 (pp. 3366-3371). IEEE.
[8] Rantzer A, Lidstrom C, Pates R. Structure Preserving H-infinity Optimal PI Control. IFAC-Papers OnLine. 2017 Jul 1;50(1):2573-6.
[9] Megretski A, Rantzer A. System analysis via integral quadratic constraints. IEEE Transactions on Automatic Control. 1997 Jun;42(6):819-30.
[10] U. Jonsson, Lecture notes on integral quadratic constraints, Dept. Math., Royal Institute of Technology, Stockholm, Sweden, 2001.
[11] Rantzer A. On the Kalman-Yakubovich-Popov lemma. Systems Control Letters. 1996 Jun 3;28(1):7-10.
[12] Andersen MS, Pakazad SK, Hansson A, Rantzer A. Robust stability analysis of sparsely interconnected uncertain systems. IEEE Transactions on Automatic Control. 2014 Aug;59(8):2151-6.